MAX-PLANCK-GESELLSCHAFT
ZUR FÖRDERUNG DER WISSENSCHAFTEN E.V.
PROJEKTGRUPPE FÜR LASERFORSCHUNG
D-8046 GARCHING bei München/Germany

The ASTERIX III High Power Iodine Laser, a System Performance Summary

G. Brederlow, R. Brodmann, K. Eidmann, H. Krause,
M. Nippus, R. Petsch, R. Volk, S. Witkowski,
K.J. Witte

PLF 5 July 1979

Diese Arbeit wurde gefördert durch das Bundesministerium für Forschung und Technologie und durch Euratom.

Abstract

The Asterix III iodine laser system is used for laser fusion-oriented target experiments. This single beam laser consists of an acousto-optically mode-locked oscillator and four amplifiers of increasing length and aperture. Asterix III is presently capable of delivering a maximum output power of about 1 TW at an energy level of up to 300 J. Its repetition rate is one shot every 10 minutes. The laser has demonstrated that it meets the requirements of high-quality laser plasma experiments. Its principle features are: excellent beam quality, freedom from non-linear self-focusing, relatively rapid repetition rate, few damage-prone optical surfaces, and relative ease of optical isolation from the target. In view of these properties the iodine laser favourably compares with other fusion lasers what also holds when additional aspects like ease and reliability of operation under high loading conditions are considered. There is still a significant potential for improving the performance of the iodine laser, especially for an increase of the overall efficiency.

1. Introduction

Experiments in laser-induced thermonuclear fusion research require high power lasers with subnanosecond and nanosecond pulse durations, good beam quality and stability, low prepulse energy, and sufficiently high efficiency. The iodine laser meets these requirements and the parameters presently achieved are compatible with or even better than those of the more advanced Nd:glass and CO_2 lasers.

High power operation of the iodine laser has already been demonstrated in several laboratories /1,2,3,4/. The first application for fusion-oriented plasma experiments for the iodine laser was in the Asterix III system built at the Projektgruppe für Laserforschung (PLF), Garching. This laser has been designed for an output power of 1.0 TW in a single beam. It became operational at the specified power in 1977. Up until the present time, the system has been used routinely in more than 500 shots for target experiments.

In the present paper a review of the basic features, construction, and performance of the Asterix III system will be given. One property of particular interest was the beam quality along the beam path in the laser. It was measured by lateral shearing interferometry, by the multiple spot method and by the diaphragm

method. Owing to the nonlinear nature of the pulse amplification and attenuation in the amplifiers and in the saturable absorber pulse shaping effects have to be expected. These effects were also investigated. In addition, the bandwidth of the laser pulse, the prepulse power and the spatial focus stability were measured. Finally the experiences with target experiments will be reported and the potential for further improvements of the laser system will be described.

2. Iodine laser characteristics

The iodine laser is a photochemical gas laser. It operates on the magnetic dipole transition $^2P_{1/2}$-$^2P_{3/2}$ of atomic iodine at 1.315 µm. The laser medium used in the ASTERIX III system is perfluoro - isopropyliodide i-C_3F_7I which decomposes upon irradiation with UV-light (λ = 280nm) in C_3F_7-radicals and excited I($^2P_{1/2}$)atoms. Both levels of the laser transition show hyperfine splitting resulting in two and four sublevels, respectively (Fig. 1). As the cross section for stimulated emission of pure i-C_3F_7I has too high a value for amplifier conditions, it has to be reduced by pressure broadening of the laser transition. For this purpose argon is added to the laser medium. This buffer gas has a sufficiently high pressure broadening constant and a low deactivation rate. According to calculations /5/ the relaxation time within the lower sublevels under typical amplifier condi-

tions is short in relation to a ns pulse, and for the upper sublevels, it is significantly longer than a ns pulse, as is confirmed by measurements /6/. Each of the two triplets arising from the F = 2 and F = 3 sublevels of the excited

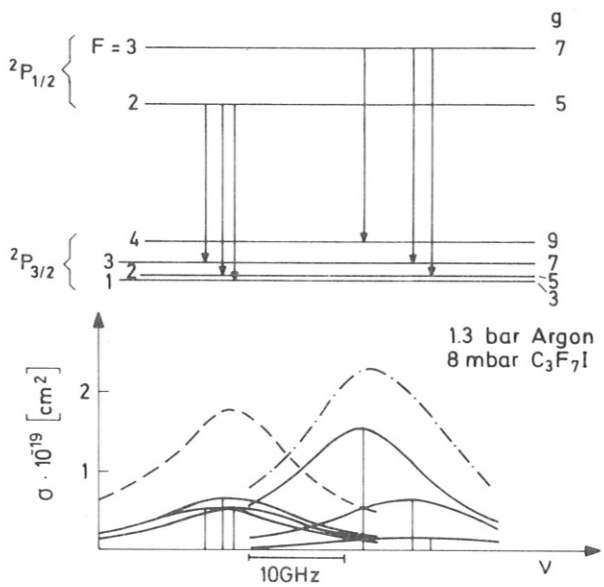

Fig. 1 Hyperfine splitting of the iodine laser levels. Lower plot shows cross sections for stimulated emission at 8 mb i-C_3F_7I and 1.3 bar argon

state can therefore be imagined as forming one homogeneously broadened line, with both lines coupled by the sublevels of the ground state. For optimum energy extraction, a pulse should therefore contain frequencies of both groups of lines. Owing to the degeneracy of the sublevels, the ultimate amplifier extraction efficiency in the saturation region is $\eta_{ext} = 0.45$,

provided that there is no access to the energy stored in the F = 2 sublevel. Ordinarily the 3-4 line is generated by the oscillator because it has the highest gain.
The partial pressure p_L of the laser medium i-C_3F_7I depends upon the diameter d of the laser tubes. Since maximum energy storage requires a large i-C_3F_7I pressure and a flat inversion profile a low pressure, a compromise has to be found. For amplifiers using a reflector geometry that does not image the flashlamps the empirical formula,

$$p_L \cdot d = 200 \text{ mbar} \cdot \text{cm},$$

yields an inversion profile with an about 40% lower inversion density at the center than at the edge of the active area. This inversion profile still guarantees a sufficient homogeneity of the energy profile of the laser pulse.

The partial pressure of the argon has to be adjusted in the amplifiers such that the small signal amplification (SSA) is below the threshold for internal parasitic oscillations. For all amplifiers this value is larger than 1000. The SSA value actually chosen must, however, be somewhat smaller in order to avoid parasitic oscillations caused by amplifier coupling. Experience has shown that the spatially averaged SSA-value of an amplifier should therefore be kept below 400.

For an active modelocked oscillator, as used in the Asterix III system, the argon pressure depends on the desired pulse duration τ . The pulse duration bandwidth dependence given by the Sigmann-Kuizenga theory is $\tau \sim (\Delta\nu)^{-1/2}$, where $\Delta\nu$ is the bandwidth of the laser transition. Its relation to the argon buffer gas pressure is given in /7,8,9,10/.

After a shot the laser medium does not completely regenerate. As a consequence, the partial pressure of the i-C_3F_7I is reduced and molecular iodine, which is a strong quencher for excited atomic iodine, is formed. Therefore it is necessary to exchange the laser medium after each shot. This is accomplished by a specially designed circulation system that can restore the correct i-C_3F_7I pressure and remove the molecular iodine from the mixture /11/ (see also chapter 3.1).

Although the radiation life time of an undisturbed excited iodine atom is 130 ms, the pumping and extraction times of the laser have to be much shorter. This is because the pump light will evaporate i-C_3F_7I and some photolytic reaction products absorbed on the walls of the laser tubes, thus causing shock waves which travel radially inwards and disturb the optical homogeneity of the laser medium. The pumping times of the laser have therefore to be in the µs region in order to prevent the shock waves from covering too large a fraction of

the amplifier cross sections before the pulse is transmitted.

3. Description of the Asterix III laser system

The schematic of the Asterix III laser is shown in Figure 2. The main components of this system are the oscillator and four amplifiers. A pulse selection system with a high contrast ratio is used to extract the pulse to be amplified. Between the second and third amplifiers a saturable absorber serves for prepulse suppression and, to a certain extent, for amplifier isolation. To prevent sensitive laser components from being destroyed by light reflected from the target and to isolate the amplifiers from each other, a Faraday rotator is installed between the third and fourth amplifier.

Several components serve for beam diagnostics, laser control and remote alignment of the laser beam. The laser is situated in a temperature ($\pm$ 1°C), and humidity controlled room. However, the space available for this laser is very restricted, the laser beam path has therefore to be folded several times.

3.1 General technical features.

Basically the oscillator and the amplifiers consist of a quartz tube, surrounded by linear flashlamps and their reflec-

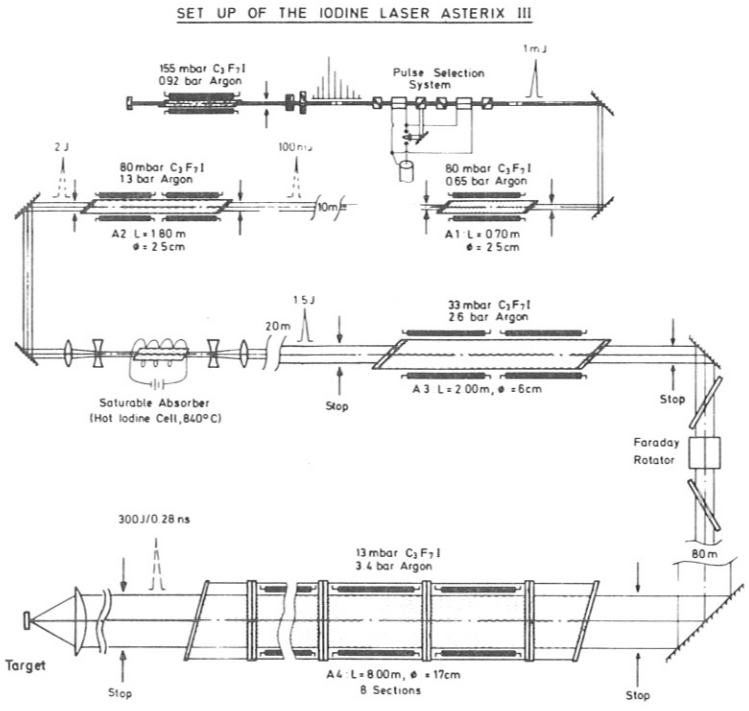

Fig. 2 Schematic of the Asterix III laser

tors. The quartz tubes containing the active media are etched on the inner surface in order to prevent focussing of the pump light by caustic effects which will impair the homogeneity of the inversion profile.

The laser medium of the oscillator and the amplifiers is exchanged by an automatic recycling system. It cleans the laser gas by condensing the photolytic reaction products in a cooling trap and replaces the expended laser medium by

passing the gas through a vessel where stored liquid i-C_3F_7I is cooled to a temperature at which its vapour pressure corresponds to the required partial pressure in the laser tubes. The replacement times range between 1 and 8 minutes.

For operation over long time intervals (several weeks) the entire circulation system has to be vacuum tight with a leak rate of 10^{-7} mbar l/sec for the oscillator and the first two amplifiers, 10^{-6} for the third amplifier and 10^{-4} for the last amplifier. The laser tubes and their recycling systems have to be evacuated to a pressure of around 10^{-2} mbar when the expended i-C_3F_7I has to be replenished.

The oscillator and the amplifiers are pumped by flashlamps made from Heralux quartz tubes (Heraeus). The lamps are filled with Xenon at a pressure of 40 mbar. Tests showed that this pressure provides the maximum pumping efficiency for iodine amplifier operation. The pumping times range from 1.5 to 11.5 µs, depending upon the tube diameter and sound speed in the laser medium.

For the oscillator and the first and second amplifiers sealed commercial flashlamps are used. These lamps have to be replaced after 1000 - 2000 shots, because the UV-yield decreases. This decrease originates from an increasing impurity level in the Xenon gas lowering the electron temperature.

The third and fourth amplifiers are pumped by specially designed unsealed flashlamps. In these lamps the Xenon has to be exchanged after 10 - 20 shots. These lamps are replaced after around 800 shots, because an increasing number of micro cracks in the quartz walls near the electrodes has then raised the probability for a lamp explosion to a value which is too high for a reliable operation.

Transparency measurements of these flashlamps revealed that the Xenon plasma is optically thick to the radiation of the iodine pumping band. This fact has to be taken into account by optimizing the reflector geometry. The reflectors for the flashlamps are made from electro-polished pure aluminum sheets (99.99% Al). Their reflectivity at $\lambda \approx 280$ nm is in the range between 80% and 90%. The reflectors of the oscillator and the first, second and third amplifiers are U-shaped. This geometry is not optimal because a relatively large fraction of the pumplight emitted in the radial outward direction and then reflected into the flashlamp is reabsorbed in the optically thick Xenon plasma. In order to make this fraction as small as possible, the reflector geometry of the fourth amplifier was improved by using W-shaped reflectors (Fig. 3) which direct the outwardly radiated pumplight by double reflection into the laser medium. They have been successfully employed for the last three years. These reflectors and a new arrange-

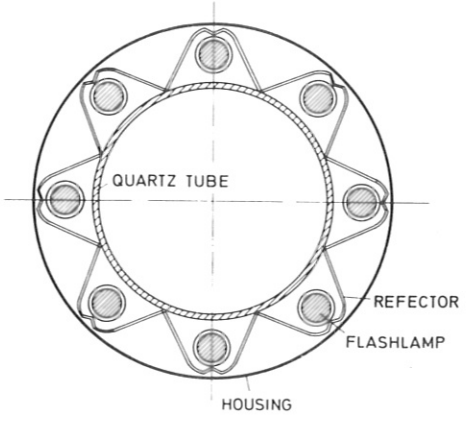

Fig. 3 Cross-section of the 4th amplifier with w-shaped reflectors

ment of the flashlamps increased the pumping efficiency by a factor of nearly two, compared with the originally U-shaped reflectors.

The flashlamps heat up the laser tubes non uniformly, thus causing the formation of non-uniform and non-constant temperature gradients transverse to the tube axis. Their orientation is mainly in the vertical direction. These gradients lead to density and hence refractive index gradients in the laser medium, which in turn induce disturbances of the directional stability of the laser beam. To prevent the formation of these gradients, the quartz tubes of the oscillator and the amplifiers have to be cooled. In the Asterix III system open-cycle air cooling is used for this purpose. The temperature gradients are controlled by thermocouples. Stable conditions could be established within 10 minutes. The air cooling system has, however, the disadvantage of gradually degrading the reflectivity of the flashlamp reflectors by dust deposition. In addition, it does not prevent the formation of ozone, which may attack the surface of the aluminum reflec-

tors. It is therefore planned to replace the air cooling by a closed loop N_2 cooling system.

3.2 Oscillator and pulse selection system.

The oscillator consists of a quartz tube with BK7 glass windows oriented at Brewster's angle. The active length of the oscillator is 85 cm, and its active diameter 0.8 cm. It is surrounded by four flashlamps and their reflectors. The flashlamps are operated in parallel, all powered by one capacitor bank of 1.1 kJ at 45 kV. The rise time of the pump light is about 1 µs. Further specifications of the oscillator are given in Table 1. The acousto-optically mode-locked oscillator using a semi-confocal resonator and operated in the TEM_{oo} mode has a length of 250 cm. The reflectivity of the output mirror is 60%. The pulse train emitted contains pulses of 0.5-0.7 ns (FWHM) duration which are exclusively on the 3-4 transition. The single pulse extracted by the pulse selection system has an energy of about 1 mJ and a diffraction limited beam divergence of 10^{-3} rad (full angle).

To achieve sub-nanosecond pulses reliably, a modulator operating in the Raman-Nath mode is used. It is powered in pulsed operation (1 ms pulse length) by a 20 W pulse having a carrier frequency of 30 MHz. A modulation index of about 3.5 could thus be obtained. The pulse selection system provides a high

T A B L E 1

	Dim.	Osc.	A_1	A_2	A_3	A_4
active length	cm	85	65	160	185	740
active diameter	cm	0.8	1.6	1.6	5.5	15.5
number of sections		2	1	2	2	8
i-C_3F_7I	mbar	155	80	80	33	13
Argon	bar	0.92	0.65	1.3	2.6	3.4
total number of flashlamps		4	4	4	16	64
active length of the flash-lamps	cm	43	65	79	92	92
inner diameter of the flash-lamps	cm	0.8	0.8	0.8	1.8	1.8
Xe pressure	mbar	40	40	40	40	40
max. operating voltage	kV	45	40	40	40	40
max. electr. energy stored per amplifier	kJ	1.1	2.6	4.4	72	288
number of circuits		1	1	1	8	32
input energy/flashlamp	kJ	0.28	0.66	1.1	4.5	4.5
current pulsewidth (FWHM)	µs	1.1	2.4	2.4	5.5	5.5
rise time of the pumping light	µs	1.0	1.6	1.6	4.2	4.2
pumping time until extraction	µs	1.5	6.0	6.0	11.5	11.5
trigger delay	µs	10.0	5.5	5.5	0	0

optical isolation of the oscillator from the amplifier chain. It consists of two Pockels cells in series and three Glan polarizers, the total attenuation of the closed system (zero voltage at the Pockels cells) being about 10^{-9}. The Pockels cells are switched by a laser-triggered spark gap.

The oscillator is mounted on a granite bench. It perfoms very reliably without requiring realignment for periods of several months. The maximum repetition rate of the oscillator is one shot every minute. So far it has been fired for several thousands shots without damage and misalignment problems.

3.3 Amplifiers

The Asterix III system comprises four amplifiers of successively increasing diameter, length and energy content. Their specifications are given in Table 1. The distances between the amplifiers are chosen such that the beam spread due to its natural divergence fills the diameter of the following amplifier. The beam diameter thereby expands over a distance of 148 m from 0.2 to 15.5 cm.

The first, second and third amplifiers consist of one quartz tube and a support for the flashlamps and the reflectors. The dimensions of the quartz tubes, the number and dimensions of the flashlamps, and the specification of the capacitor banks are given in Table 1.

The first and second amplifier each have an active diameter of 0.8 and 1.6 cm and an active length of 65 cm and 160 cm respectively. The Brewster angle windows consist of 1.0 cm thick BK7 plates. Each amplifier is pumped by four flashlamps operated in parallel and charged by one spark gap. Their flashlamp circuits are nearly critically damped. The rise time of the pump light is 1.6 µs for both amplifiers, and the current pulse width 2.4µs (FWHM). The electric energy of the capacitor banks at 40 kV is 2.6 kJ and 4.4 kJ. It is converted to a maximum stored optical energy in the amplifiers of 12 J and 20 J, respectively. Both amplifiers are released after a pumping time of 6 µs.

The third amplifier has an active diameter of 5.5 cm and an active length of 185 cm. The BK7 windows placed at the Brewster angle are 2.0 cm thick (for further data see Table 1). Whereas in the first and second amplifier an argon buffer gas pressure in the range of 1 bar reduces the mean small signal amplification of an amplifier to a value of around 100, in the third amplifier a buffer gas pressure of 2.6 bar has to be employed to achieve the same gain level.

The flashlamps of the third amplifier are arranged in two sections, each having 8 flashlamps and reflectors. Two flashlamps are always operated in parallel and charged by one spark gap.

The total energy stored in the capacitor bank of each section is 36 kJ at 40 kV. The current has a pulse width of 5.5 µs (FWHM) and the rise time of the pumping light is 4.2 µs at 40 kV. Up to 280 J optical energy are stored in the third amplifier. This amplifier is released after a pumping time of 11.5 µs.

In the fourth amplifier the essential energy gain of the pulse occurs (Fig. 4). The design of this amplifier differs

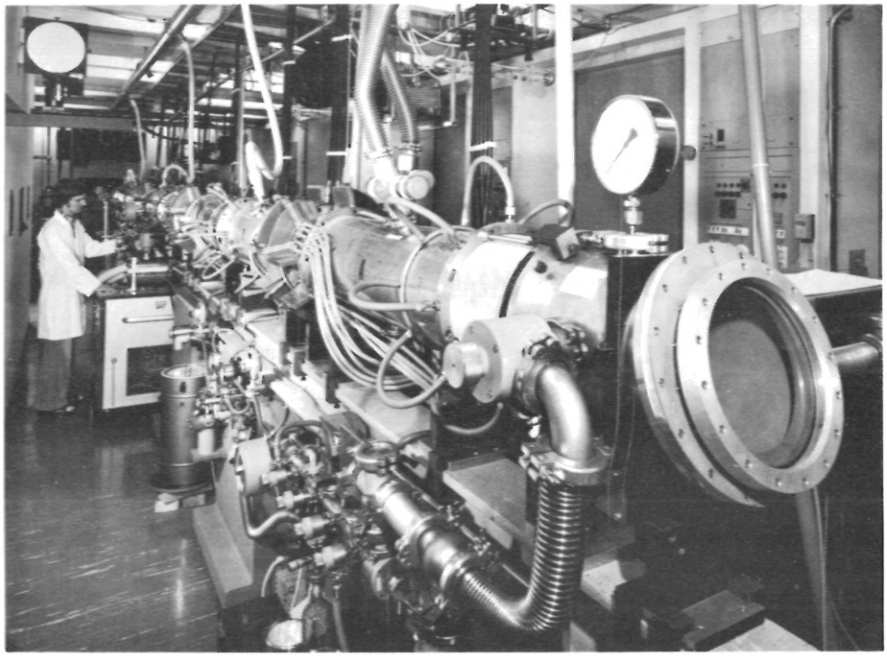

Fig. 4 Fourth amplifier of Asterix III

from the preceding ones. It is assembled from eight individual sections. Each section is composed of an inner quartz

tube etched on the inner surface, a stainless steel housing and eight flashlamps with their reflectors mounted between the quartz tube and the housing. The active diameter of this amplifier is 15.5 cm and its total active length 740 cm (further data in Table 1). The argon buffer gas pressure for σ-reduction is up to 3.4 bar. Because of this high pressure and the large aperture the windows could no longer be placed at the Brewster angle. At this angle the plates would become too thick, otherwise the high pressure would bend them and thus the optical quality of the laser beam would be impaired. The windows were here installed at an angle of 35°. At this angle a thickness of 3.5 cm provides sufficient mechanical stability. The windows have anti-reflective coatings to reduce the reflection losses and to increase the threshold for the appearance of internal parasitic oscillations. Only protected hard coatings could be used, otherwise a chemical reaction of the coating material with the photolysis products of the laser medium would take place.

The electrical pumping circuit of one section of the fourth amplifier including the flashlamps is identical with that of one section of the third amplifier. The total energy stored in the eight capacitor banks of this amplifier is therefore 288 kJ at 40 kV. It is released after a pumping time of 11.5 µs. The total stored optical energy at 40 kV is up to 1.8 kJ. The threshold for internal parasitic oscillations is at a

SSA value of about 10^4. This value could only be achieved, when the inner surfaces of the quartz tubes are etched, the windows are antireflection coated and a light trap is installed close to the windows.

The inversion profile of this amplifier was derived from measurements of the small signal amplification and the stored optical energy at i-C_3F_7I partial pressures of 8 and 15 mbar (Fig. 5). For laser operation an intermediate partial pres-

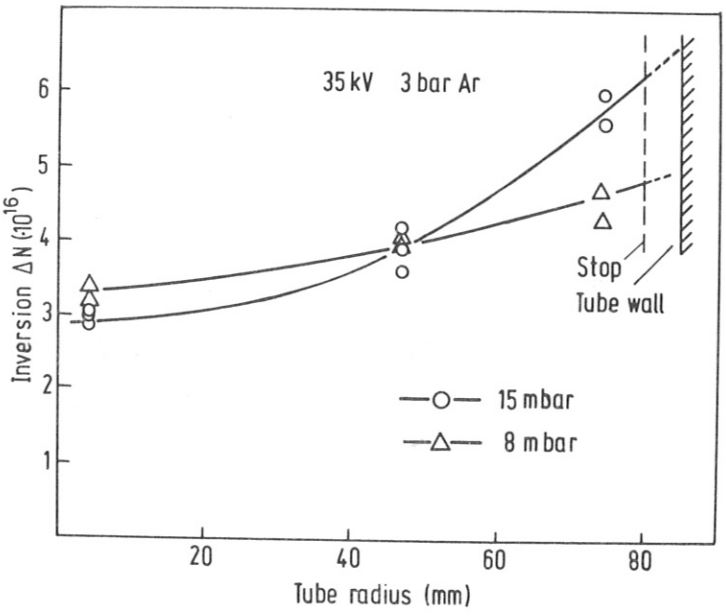

Fig. 5 Inversion density profile of the fourth amplifier at a C_3F_7I-pressure of 8 mb and 15 mb

sure of 13 mbar provides an acceptable gain profile. The inversion density measured in a pumping energy range from

160 - 290 kJ (30 - 40 kV) shows a linear increase with the pumping energy. This result indicated that for the pumping process nonlinear loss mechanisms are not significant in the energy range investigated.

3.4 Optical isolation of the amplifiers and prepulse suppression.

To provide optimal energy extraction efficiencies the pulse to be amplified should saturate the amplifiers as much as possible. This requirement calls for high small signal amplification exceeding the actual energy amplification by several orders of magnitude. In the amplifier chain, high threshold values for parasitic oscillations therefore have to be maintained. Because of the high small signal amplification, however, special precautions have to be taken to prevent prepulse signals (amplified at the full small signal gain) from exceeding such a power level that sensitive targets are damaged before the main pulse strikes it.

The simultaneous requirements of high threshold values for external parasitic oscillations and low prepulse energies can be met by sufficient optical decoupling of the amplifiers. The methods used for this purpose in the Asterix III system are as follows:

a) Large distances decouple adjacent amplifiers, because parasitic oscillations result from diffuse reflections at windows and other external structures. Therefore solid angles of less than 1 - 2 mrad of an amplifier as seen from the adjacent amplifiers provide good decoupling. These angles are readily obtained in the Asterix III laser.

b) A further decoupling of the amplifier was obtained by placing stops at the entrance and exit of each amplifier with diameters chosen such that the zones covered by the shock waves were blocked. As these zones have the highest inversion density, the stops impair the tendency of the amplifiers to prelase. (In addition, they prevent disturbance of the beam quality by an interaction of the laser beam with the area covered by the shock waves).

c) The Faraday rotator, placed between the third and fourth amplifiers also serves for optical decoupling. It reduces the tendency for prelasing and prevents sensitive optical components from being destroyed by amplified light reflected from the target. The backward-foreward extinction ratio of this Faraday rotator approximately is 400.

d) The pulse selection system with two Pockels cells installed in series has a total attenuation of the closed system of 10^{-9}, thus providing excellent optical isolation

between the oscillator and the amplifier chain so that the contribution to the prepulse energy caused by the leaking of the pulse selection system is at a level where it is not harmful to the target.

e) A saturable absorber placed between the second and third amplifiers attenuates all contributions to the prepulse energy (see chapter 4.2). It diminishes the small signal amplification of the total laser system by a factor of nearly 10^{-3}. This absorber not only reduces the prepulse energy but also improves the optical isolation of the amplifiers. The isolation capability is, however, impaired because the absorption bandwidth of the absorber (500 MHz) is much smaller than the bandwidth of the amplifiers (5 - 8 GHz).

To achieve saturation the laser transition is used in absorption /12,13/. The atomic iodine in the ground state is produced by thermal dissociation of I_2 in a hot cell ($T \simeq 800°C$). The saturation characteristic shown in Fig. 6 was measured for ns pulses. Owing to the nonlinear nature of the absorption pulse shaping effects such as steepening and shortening of the pulse take place /14/. Nonlinear effects such as multiphoton absorption or self-focussing were not observed.

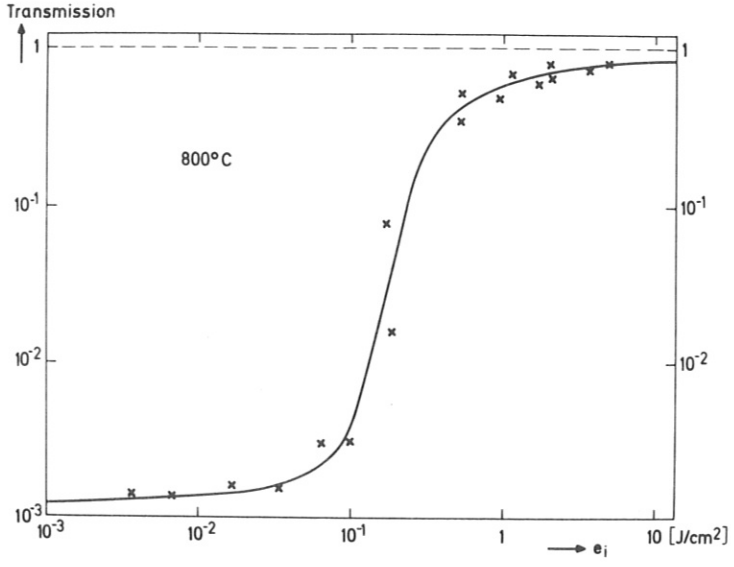

Fig. 6 Transmission of a saturable absorber cell (l = 40 cm, Ø = 2.5 cm) filled with 50 mg I_2 at a temperature of 800°C

All these measures for optical amplifier decoupling and prepulse reduction provide the conditions in the Asterix III system that an overall small signal amplification of all amplifiers of about 10^9 could be sustained at a sufficiently low prepulse level, the energy amplification then being around $5 \cdot 10^5$.

3.5 Laser alignment and maintenance.

The alignment procedure is based on the alignment of He-Ne laser beams coinciding with the iodine laser beam. In the

Asterix III system three He-Ne lasers are used for this purpose (Fig. 7). The first one is for the adjustment of

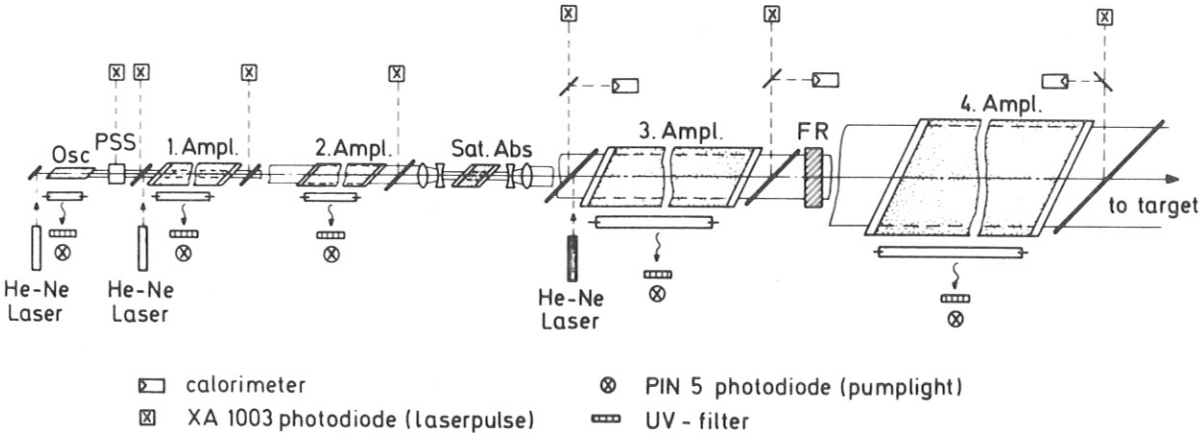

Fig. 7 Control system of the Asterix III Laser

the oscillator and the beam path through the first amplifier. The second one serves for beam alignment from the first amplifier to the saturable absorber. Since the He-Ne laser beam is partially absorbed in the saturable absorber, a third laser is inserted in front of the third amplifier.

To check the state of alignment fiducial marks are placed in the beam path at different positions. In addition, since mirrors with dielectric coatings are used to fold the beam path, the transmitted He-Ne laser beam is positioned behind

these mirrors by an array of photodiodes. If necessary the laser beam is then easily adjusted by remote mirror control.

To control the laser operation, the timing and the time behaviour of the UV pumplight of the oscillator and the amplifiers is measured by PIN5 diodes through filters (λ_{max} = 276 nm; $\Delta\lambda$ = 12 nm (FWHM)) and monitored by an oscilloscope. In addition, the output energies of every amplifier are recorded by digital joulemeters (Gen-Tec), by germanium diodes and by diodes with proximity focussed S_1 cathodes (XA 1003, Valvo) (Fig. 7). Information on the shape of the laser pulse at the output of the first amplifier is provided by a XA 1003 diode (rise time: 400 ps with Tektronix 519). At the output of the fourth amplifier the pulse shape is recorded by a EPL-ICC-512 streak camera with a S1 cathode (selected sensitivity for 1.3µm) and a time resolution of 20 ps.

3.6 Stability and reliability of laser operation.

The requirements for a reliable and reproducible laser operation are besides stable beam alignment and reproducible conditions regarding the status of the laser medium and the electrical energy stored in the capacitor banks, reproducible working of the electrical network of the oscillator, the amplifiers and the Faraday rotator.

In the Asterix III system these requirements could be met. The first three are reliably satisfied before firing the laser and the last one, the functioning of the electrical system, has a probability of misfiring and failure of less than 2%. These misfirings also cover shots with a jitter exceeding 0.5µs in the timing of the pumping process of the oscillator and the amplifiers.

Reproducible laser pulse properties also call for stable operation of the oscillator and the pulse selection system. In the Asterix III laser the probability of improper functioning of these two systems is about 5%. This probability is here defined as the fraction of shots consisting of double pulses or pulses which differ from the average values of the pulse energy and duration by more than 50%.

Of importance is also a stable pumping efficiency of the amplifiers. In the Asterix III system this efficiency decreases under certain conditions with increasing shot number. Measurements, not only performed with the Asterix III system /15/, demonstrated that this decrease is mainly due to the fact that a pumplight absorbing layer forms on the inner surface of the quartz walls of the amplifiers. As shown in Fig. 8, in an amplifier with a new quartz tube, there is a steep decrease of the output energy within the first 40 shots and then

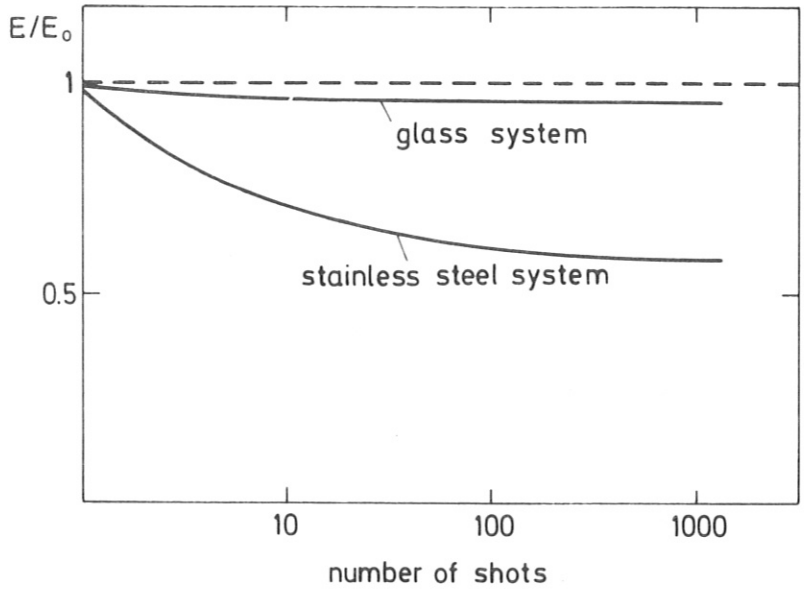

Fig. 8 Normalized output energy as a function of the shot number for an amplifier with a stainless steel or a glass circulation system

it levels off with increasing shot number. This nearly stable behaviour at higher shot number is caused by a certain equilibrium between deposition and vaporization of the absorbing layers.Investigations performed in a separate experiment revealed that this layer is formed by a compound originating from the reaction of photolysis products of the i-C_3F_7I molecules with the stainless steel wall material of the circulation system. By replacing the stainless steel by a glass or aluminum circulation system pumplight absorbing deposits were then no longer be detected (Fig. 8). The slight

5% decrease of the output energy during 1000 shots is due to the fact that the pumping efficiency of the flash lamp decreases.

The stainless steel circulation systems of the Asterix III laser will be replaced by a glass system for the first and second amplifiers and by an aluminum system for the third and fourth amplifiers. The laser can then be expected to keep the high energy output level for a larger number of shots corresponding to the upper curve in Fig. 8.

4. Power and energy characteristics.

The Asterix III laser is now routinely employed for target experiments. The diagnostics in use to investigate the pulse properties are shown in Fig. 9. Of primary interest are the energy and the shape of the laser pulse, its prepulse energy and power, the beam quality (focussibility), the pulse bandwidth (temporal smoothness), the directional stability of the beam, its energy profile and the effort necessary to isolate the laser from the target.

4.1 Output energy and pulse length.

The maximum optical energy stored in the last amplifier is 1.8 kJ at 40 kV if the wall of the quartz tube is free from

absorbing layers. When, however, the target experiments were started, this energy had gone down to about 1.1 kJ owing to amplifier contamination. An output energy of 300 J (40 kV) was then achieved. As the entire system is pumped

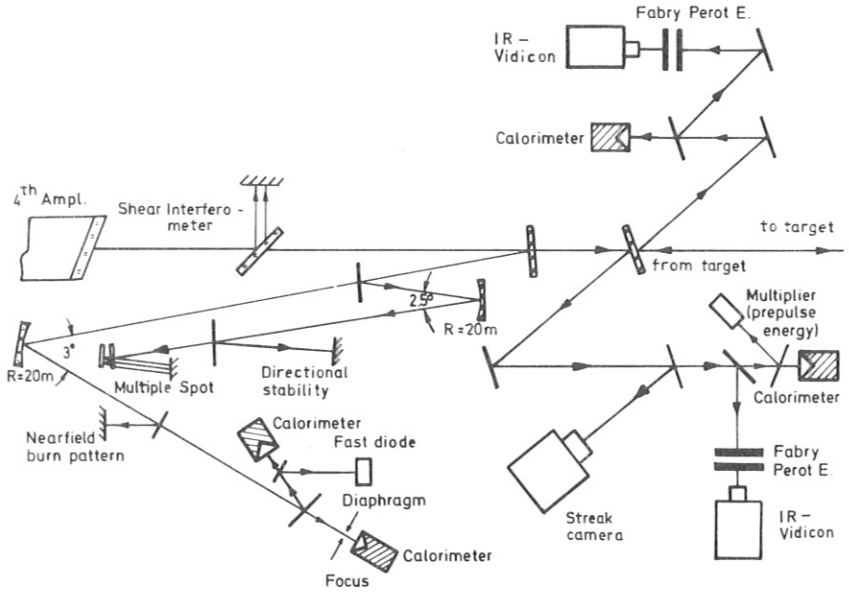

Fig. 9 Schematic setup of the diagnostics

with an energy input of 370 kJ, the outpulse pulse energy of 300 J then corresponds to an overall efficiency of $\eta_o = 0.08\%$.

The mean pulse duration measured with a streak camera at the output of the fourth amplifier is 280 ps. The planned output power of 1 TW could thus be achieved. During the amplification process the pulse shape did not stay constant. Substantial pulse steepening and shortening occurs in the sa-

turable absorber and to a minor degree in the saturation region of the third and fourth amplifiers /14/. As shown in Fig. 10 the pulse length decreases from 0.5 - 1.0 ns at

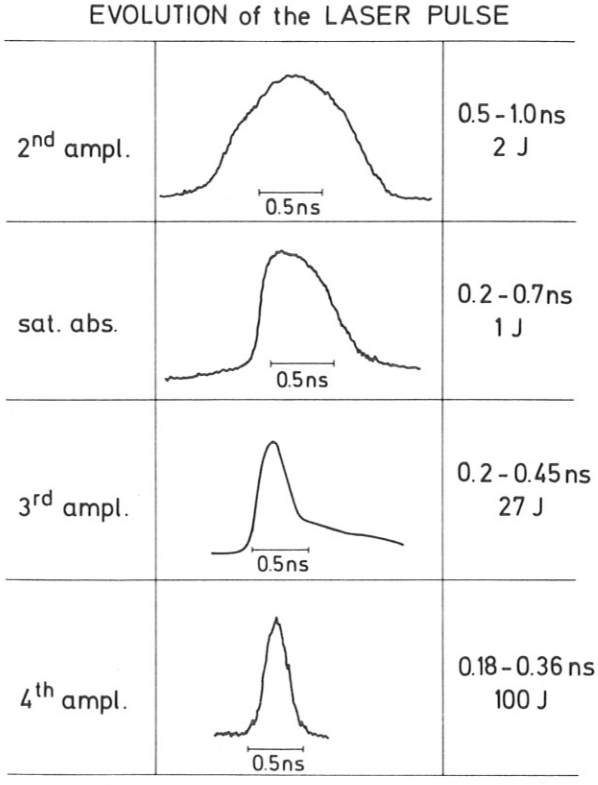

Fig. 10 Time evolution of the pulse along the chain (streak camera measurements). Right column tabulates the range of observed pulse lengths.

the exit of the second amplifier to 0.18 - 0.36 ns (FWHM) after the fourth amplifier. Since the iodine laser does not need any spatial filter to control the beam quality no pulse length restrictions arise. With the Asterix III laser experi-

ments have been performed so far in the pulse range from 180 to 800 ps. In this range the output pulse energy is not strongly dependent upon the pulse duration. This behaviour can also be extrapolated into the region of some ns. At pulse durations exceeding 10 ns an increase of the output energy due to hyperfine relaxation processes of the upper sublevels can be expected. For pulses below 150 ps, the output energy level has to be reduced because of damage threshold limitations of the coatings.

Information on the reliability and reproducibility of the system is given in Fig. 11, where the output energies of the

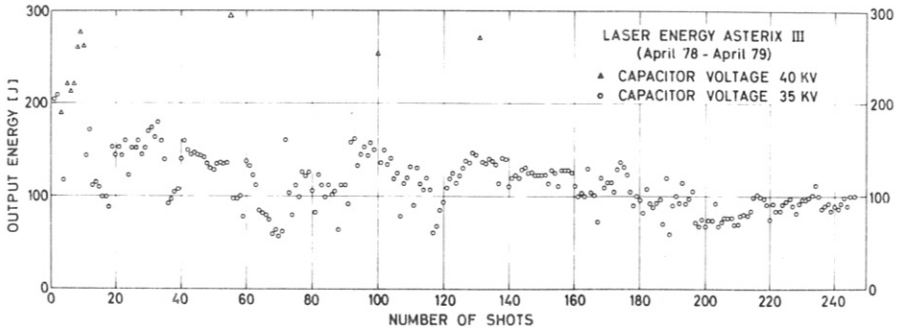

Fig. 11 Output energies of the Asterix III laser at charging voltages of 35 kV and 40 kV

last 246 shots are plotted versus the shot number. Most of these shots are taken at a capacitor voltage of only 35 kV since the requirements of the target experiments were met at an energy level of about 100 J. But some shots were also performed at the full pumping energy of 370 kJ (40 kV) yielding, with the already absorbing layers on the amplifier walls an output energy of up to 300 J.

The minima in the output energies at shot numbers 35, 71, 117 and 197 are due to the fact that the liquid i-C_3F_7I in the storage vessels of the third or fourth amplifiers were exhausted. (No direct monitoring capabilities for the liquid i-C_3F_7I supply were in the first design of the circulation systems available). The other irregularities in the pulse energies are mainly caused by incorrect alignment of the system or by insufficient regeneration of the laser medium.

Information on the reproducibility of the output pulse duration are specified in the histogram in Fig. 12 based on streak camera measurements. The majority of the pulses range here from 180 to 360 ps the mean value being 280 ps. The few values higher than this are correlated with oscillator malfunctions.

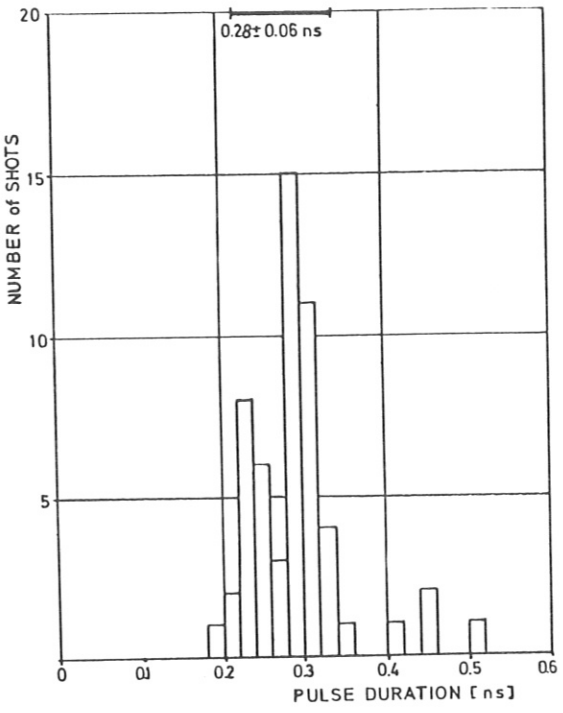

Fig. 12 Histogram of the quantity of pulses versus pulse length

4.3 Prepulse power.

The prepulse power is measured with a photomultiplier (Typ: 150 CVP, Valvo) at a power contrast ratio of 3×10^{-10} and a rise time of 3.5 ns (Fig. 9). The power detection threshold is below 100 W and hence the energy detection threshold due to the pumping time of around 10µs below 1 mJ.

There are several contributions to the prepulse power. First

there may be background radiation of the oscillator which passes the pulse selection system during its opening time (14 ns). This contribution could not yet be accurately measured because of the limitations in the time resolution of the detection system. The target experiments show, however, that it does not damage the target or impair the diagnostic capability before the arrival of the main pulse.

The second contribution to the prepulse power is due to the leaking of oscillator pulses through the closed pulse selection system. But since this system has a high contrast ratio, this leaking power is in the range of 1 kW. Because of the sub-nanosecond pulse duration its contribution to the prepulse energy is only around 2 µJ.

The third contribution is caused by amplifier spontaneous emission and is of minor importance because of the small Einstein coefficient for spontaneous emission. For the Asterix III system its contribution was calculated to be less than 100 W.

The fourth and major contribution to the prepulse power may result from prelasing of the amplifiers. However, prelasing and amplified spontaneous emission of the laser medium is below the detection threshold at 100 W in the two cases with and

without a target. Even with a high reflective plane metal target carefully aligned in the focus of the target lens at normal incidence no increase of the prepulse power could be detected. The total prepulse energy including all contributions is less than 1 mJ.

4.3 Beam quality.

There are several sources which may lead to wave front distortions of the laser beam and therefore to deterioration of the beam focussing. Two groups can be distinguished. The first one covers the intensity independent wave front distortion and the second the intensity dependent one.

The intensity independent impairment of the wavefront can be caused by three sources. First, there is the disturbance introduced by imperfect optical components such as windows, mirrors, polarizers, lenses etc. This can in principle be corrected. The second contribution originates from air turbulence along the beam path. It will be reduced or even vanish when the beam path is shielded. The third source arises from spatially inhomogeneous pumping which leads to inhomogeneities in the photolysis rate and, in present amplifiers, to a slightly concave inversion profile /16/. This inhomogeneity produces a temperature gradient resulting in a pressure gradient in the radial direction, which in turn generates a radial com-

pression wave. In the area not covered by the shock wave, a gas density gradient and hence a refractive index gradient directed perpendicular to the axis of the amplifier is then established. It leads to a whole beam expansion. Calculations performed for the Asterix III system revealed that this effect may cause a phase variation of up to one wavelength across the radius of the last amplifier. Although this distortion does not introduce a serious beam quality degradation, it can be reduced by using a buffer gas with a high molecular weight, by more homogeneous pumping or by introducing a phase correction plate.

The second group, the intensity dependent wave front distortion can originate from two sources. The first one refers to an excessively high value of the nonlinear index of refraction n_2 of laser components placed in the beam path. In the case of intensity gradients in the beam profile, the wave then influences its own index of refraction, and time-dependent focussing or defocussing of the beam occurs. A measure of this effect is the value of the beam breakup integral B:

$$B = k \int_0^l I(l)\, n_2/n_0\, dl$$

where k is the optical wave number, n_2 the nonlinear and n_0 the normal index of refraction and I(l) the beam intensity at

the position 1. To maintain a good beam quality, a value of 2.5 should not be exceeded by the beam breakup integral/17/. A value of 1.4 was calculated for the total Asterix III system at 500 J output energy and 0.5 ns pulse duration (target lens included). This low value is due to the fact that the n_2 of the laser medium itself and the air in the beam path is about a thousand times smaller than that of glass. Therefore it is mainly the glass components that contribute to the B-integral. However, in this case their influence is too small to impair the beam quality.

The second intensity dependent wave front distortion may arise from spatially-inhomogeneous gain saturation. The anomalous index of refraction $n(\nu)$ at a frequency ν close to the line center frequency ν_0 is given by

$$n(\nu) = n_0(\nu_0) + \frac{(\nu - \nu_0)}{2\pi\Delta\nu} \lambda\, g(\bar{I}(t))\; L(\nu - \nu_0)$$

where $\Delta\nu$ is the linewidth (FWHM), $g(I(t))$ the saturable gain coefficient and

$$L(\nu - \nu_0) = \frac{(\Delta\nu)^2}{4(\nu - \nu_0)^2 + (\Delta\nu)^2}$$

Wave front distortions therefore result when grad $[g(I(t))] \neq 0$ transverse to the beam direction. A spatial and temporal variation in the saturation behaviour will then occur, result-

ing in a whole beam lensing effect. An estimation of the influence of this effect on the wave front of the last amplifier of Asterix III gave a phase variation of less than one wave length across the radius /18/.

The beam quality of the Asterix III pulse was determined by a measurement of the focussibility of the laser beam, using the multiple-spot and diaphragm methods (Fig. 9). In Fig. 13

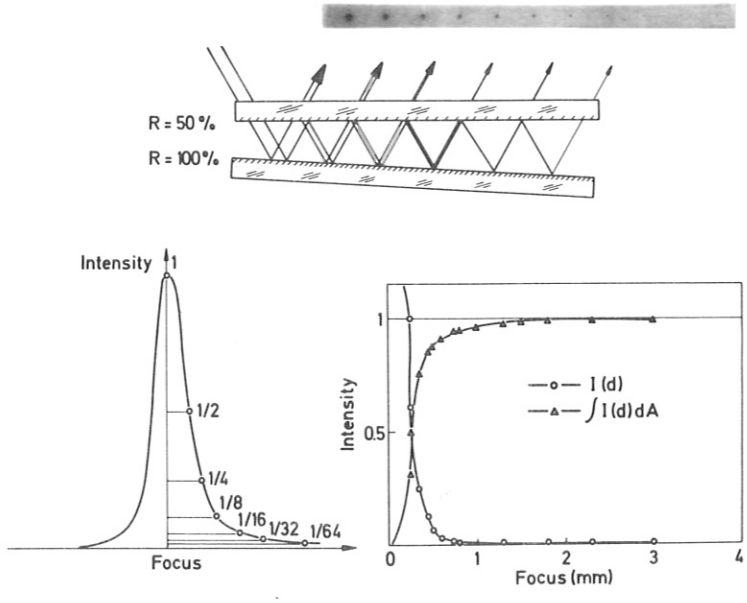

Fig. 13 Scheme of the multiple-spot method

the scheme of the multiple spot method is shown with an intensity profile recorded at the exit of the third amplifier. The results of the multiple-spot and the diaphragm method

agreed within the measuring accuracy. They are shown in Fig. 14, where the ratio of the measured focus spot size

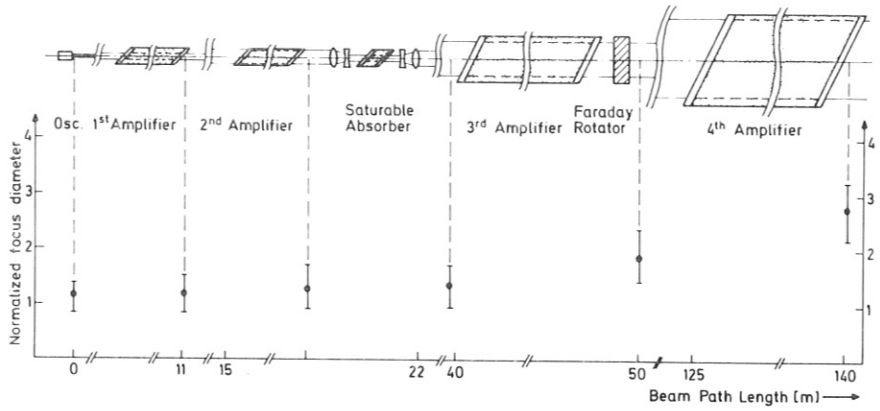

Fig. 14 Relative focussed spot size at various locations along the laser chain

is plotted versus the beam path length. The ideal reference spot size behind the oscillator and the first amplifier is the spot size of a Gaussian beam, and behind the second, third and fourth amplifiers an Airy spot size because of the more rectangular intensity profile of the beam. The focus spot size was measured at the exit of the fourth amplifier to be 2 to 3 times the ideal one. This means that an ideal f/2 lens can focus the beam to a spot size of around

30μm. With the full system in operation the power dependence of the spot size at powers of 0.2 and 0.7 TW was also measured. No power dependence was detected. For this reason and because the output beam quality did practically not change, regardless of whether the fourth amplifier was fired or not, the reduction of the beam quality has to be ascribed to intensity independent influences. Unlike the Nd laser there are no contributions of nonlinear effects of the laser medium and of optical glass components. The contribution of the anomalous dispersion at inhomogeneous gain saturation has practically no influence either.

The beam quality reduction along the beam path may be caused by an imperfect quality of optical components in the beam line or by optical inhomogeneities in the laser medium or the air of the beam path. To investigate these effects, lateral shearing interferograms were taken at different positions of the laser system. Fig. 15 shows such an interferogram recorded in the horizontal direction of shear at the exit of the third amplifier. The wavefront distortion here is less than one wavelength. In the vertical direction it is of the same order of magnitude. Fig. 16 represents an interferogram taken in the horizontal shear direction at the exit of the fourth amplifier. Here the maximum wave front distortion is up to one wavelength. The interferograms of several shots indicate that the wave front disturbance is essentially of a random nature because the spatial deviations from a straight line differ

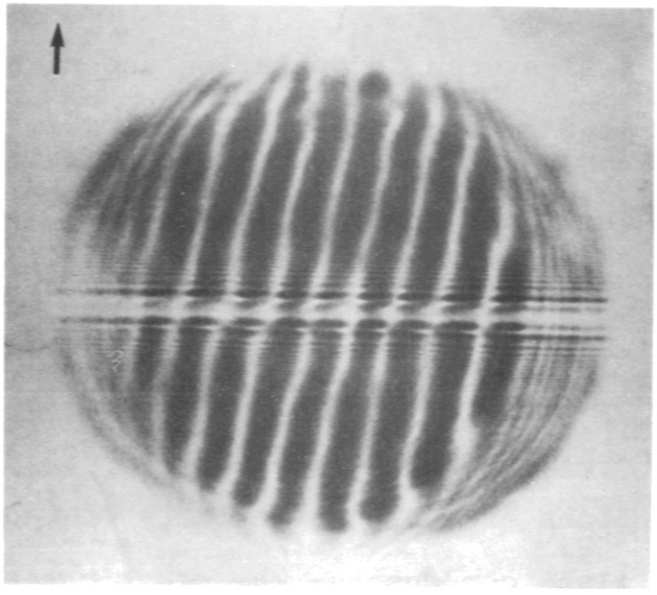

Fig. 15 Lateral shearing interferogram after the third amplifier

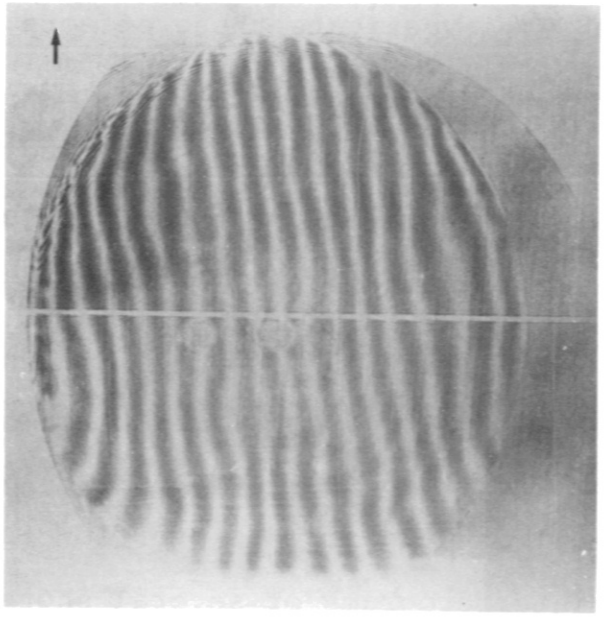

Fig. 16 Lateral shearing interferogram after the fourth amplifier

from shot to shot. The disturbances therefore can only originate from random optical inhomogeneities present in the laser medium or in the air beam path. A comparison with and without the fourth amplifier in operatin again confirms that the operation of this amplifier practically does not introduce additional wave front distortions. The beam quality reduction after the third amplifier must therefore be mainly ascribed to gasdynamic disturbances along the beam path between the third and fourth amplifier. These distortions of the wave front can be avoided by shielding the beam path, so that a further improvement of the beam quality is to be expected.

4.4 Energy profile.

The beam quality achieved in the Asterix III system implies a smooth and symmetric beam profile without any strong irregular structures. This expectation is confirmed by the near field beam photograph taken at a distance of 10 m from the exit of the fourth amplifier (Fig. 17). This qualitative picture of the beam energy profile shows a soft symmetric structure with Fresnel rings, originating from the hard stops placed at the entrances and the exits of the amplifiers. These rings will, however, not impair the focussibility of the beam. To reduce the loading of the coatings by the Fresnel rings it is nevertheless planned to replace the hard stops by soft apertures.

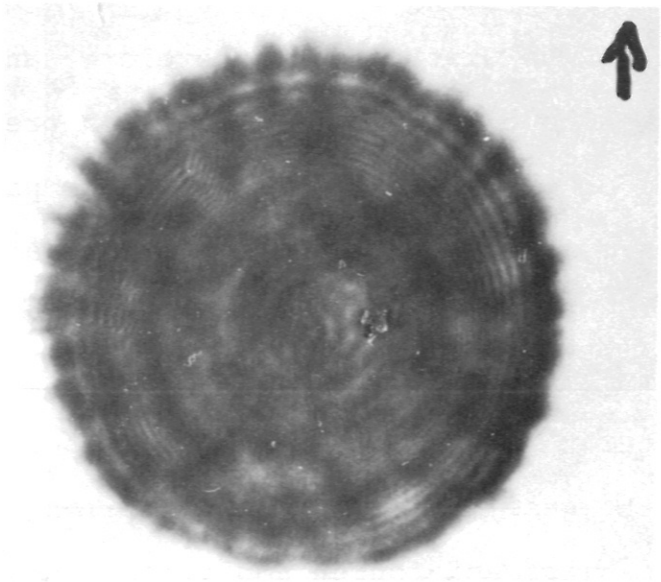

Fig. 17 Qualitative picture of the beam energy profile at the exit of the fourth amplifier

A profile similar to the near field is also recorded by hypersensitized Koda I-Z-plates in a plane equivalent to a position 400 µm ahead of the focus of the f/2 target lens. Fig. 18 shows the calibrated photometer curve of the profile. Again a symmetric Fresnel pattern can be observed and according to the inversion profile of the amplifiers the energy distribution shows a convex profile, its maximum energy being twice of its mean value.

4.5 Pulse bandwidth.

It had to be further investigated whether the requirements

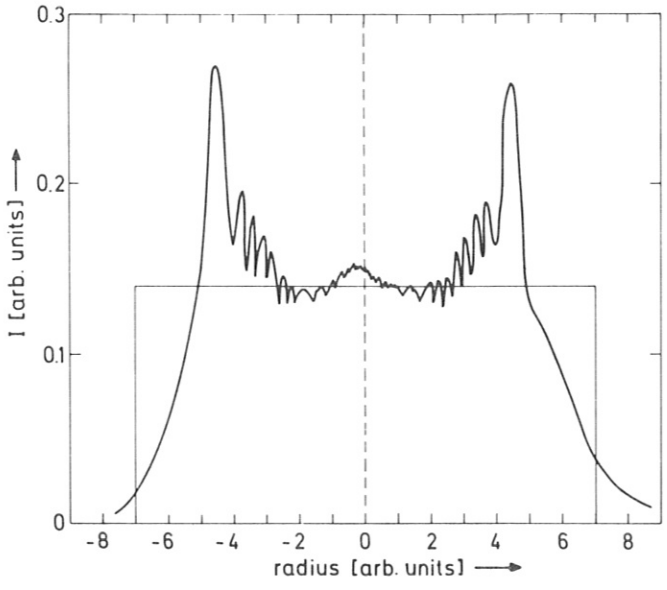

Fig. 18 Calibrated photometer curve of the energy profile in an equivalent plane 400µm ahead of the focus of the f/2 target lens

of the target experiments regarding the temporal pulse smoothness are met by the iodine laser. For this purpose bandwidth measurements are performed with a Fabry- Perot interferometer. The sub-nanosecond pulse has been investigated using spaces between the interferometer plates in the range from 1 cm to 12.5 cm. The interferogram is recorded by an infrared vidicon. Its evaluation yielded a pulse bandwidth of about $\Delta\nu$ = 2 GHz at a pulse length of about t_p = 280 ps. Since the product $t_p \cdot \Delta\nu$ is about 0.6, the iodine laser pulse cannot have any substructure.

This conclusion is additionally supported by pulse shape measurements with a EPL ICC 512 streak camera at a time resolution of 20 ps. The streak photographs showed a temporally smooth pulse without any substructure.

4.6 Spatial focus stability.

The shot-to-shot stability of the laser focus position is of importance for laser plasma experiments. Focus fluctuations in the axial beam directions can be caused in the amplifiers by a non constant whole beam lensing effect originating from inhomogeneous pumping or spatial non-uniform saturation. Measurements performed with a f/2 lens showed that the axial focus position remains within the measuring accuracy of $\pm$ 40µm at the same position irrespective of whether all the amplifiers were fired or only individual ones.

Focus position fluctuations transverse to the beam direction can originate from an imperfect mechanical stability of mirrors and lenses or by changing the transverse gas density and hence refractive index gradient in the amplifiers (see chapter 3.1). These gradients, originating from flashlamp heating, cause beam deflections. First measurements with the laser yielded a much stronger beam deflection in the vertical direction than in the horizontal direction. This stronger deviation in the vertical direction correlates quantitatively with the calculated deviations based on mea-

sured temperature gradients. By gas cooling of the amplifier walls this effect could be noticeably reduced. Under present conditions the centre of the focal spot moves by using a f/2 lens in the horizontal direction in a region of $<$ 20% and in the vertical direction in a region of $<$ 30% of the focal spot size. The directional deviations of the laser beam are therefore $<$ 20µrad and $<$ 30µrad, respectively.

4.7 Target isolation.

The target experiments demonstrated that the target did not increase the tendency to prelase. In addition, it turned out that the isolation of the iodine laser against target back reflection can be achieved with no great effort. Bandwidth measurements of the reflected light performed with a Fabry-Perot interferometer yielded spectrally broadened ($\Delta\lambda \simeq 1$ nm) and shifted light. As only a small fraction of this light falls inside the amplification bandwidth of the laser medium($\Delta\lambda \simeq 0.15$ nm), there is only a very small amplification of the back-reflected light by the residual inversion stored in the amplifiers. The Asterix III laser therefore needs only one Faraday rotator in order to prevent damage to sensitive laser components by the back-reflected light.

5. Potential for improvements.

The target experiments performed with the Asterix III system have proved the feasibility of the iodine laser for plasma experiments /19,20/. Regarding the pulse properties, the prepulse power, the repetition rate and the reliability of the laser system all requirements have already been met. Although there is still potential for improving some of these properties, it seems to us more useful to increase at first the output energy of the laser. This can be achieved by increasing the extraction efficiency of the optical energy stored in the amplifiers. This efficiency can be enlarged because the pulse to be amplified travels still too much in the small-signal region. This fact is demonstrated in Fig. 19, where the stored optical energy and the in- and output-energies of the four amplifiers are plotted versus the electric pumping energy. The dotted line shows the maximum extractable energy (η_{ext} = 45%) when the pulse always propagates in the saturation region. The solid line has been calculated by using an efficiency for the conversion of stored electric into stored optical energy at a value of η_{so} = 0.4%. Only in the fourth amplifier the pulse approaches the saturation region, but still the extraction efficiency is about half of its maximum attainable value. This deficiency is due to the fact that the matching of the amplifiers is inadequate.

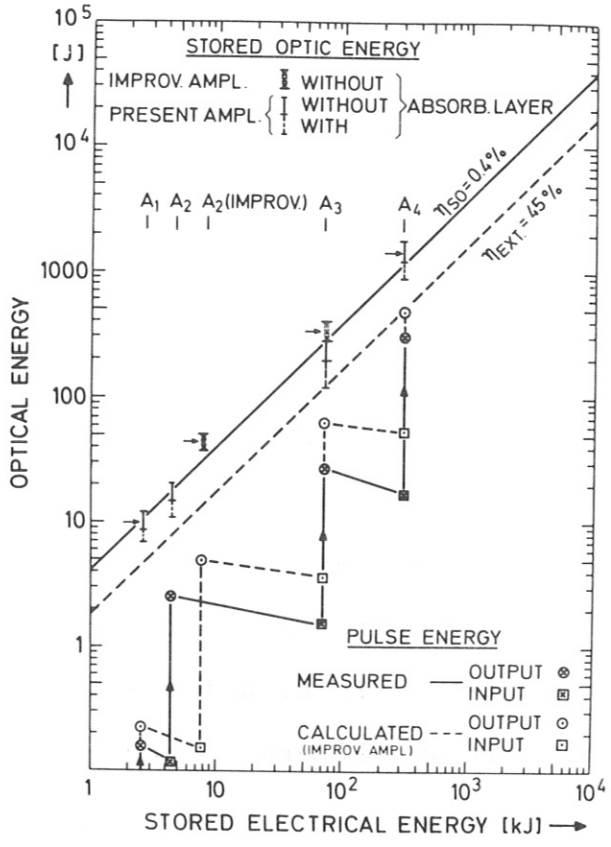

Fig. 19 Optical energy of the amplifiers as a function of the electrical bank energies

It will be improved by increasing the pumping energy of the second amplifier and raising the pumplight coupling efficiency of the second and third amplifiers.

The range of the stored optical energy of the amplifiers with no pump light absorbing layers present is indicated in Fig. 19 by solid bars. It can be seen that for the

fourth amplifier the efficiency for the conversion of the electrical into stored optical energy is above the $\eta_{l\,so}$ = 0.4% line, whereas those of the other amplifiers are below it. This difference is mainly due to the fact that for the fourth amplifier the pumplight coupling efficiency is higher than that of the other amplifiers because of the more refined reflector geometry (see chapter 3.1). However, with absorbing layers at the amplifier walls the conversion efficiencies of all amplifiers are below the $\eta_{l\,so}$ = 0.4% line (dotted bars). The improvements planned for the second and third amplifiers will raise the stored optical energies of these amplifiers to a range which is indicated by cross hatched bars.

The output energies of the amplifiers of the improved version of the Asterix III system have been calculated by using the Frantz-Nodvik formula /21/ and taking into account the transmission losses in the amplifier chain. The calculations are based on the stored optical energies indicated in Fig. 19 by an arrow. This calculation method is described in /22/. Its accuracy, checked with the Asterix III system and other experiments, was found to be satisfactory. The results of these calculations are plotted in Fig. 19. They indicate that the pulse now travels more closely in the saturation region. Therefore an increase of the laser output energy to the range of 500 J has to be expected.

6. Conclusion.

Until now the Asterix III laser has been applied for more than 500 shots for laser target experiments. These measurements have clearly demonstrated the feasibility of the iodine laser for laser fusion oriented plasma experiments.

The Asterix III laser has achieved the desired output power of 1 TW at an energy of up to 300 J and a pulse length of 180 - 360 ps, the repetition rate being one shot every ten minutes. The pulse energy corresponds to an overall efficiency of $\eta_o = 0.08\%$.

This laser meets all the requirements of laser plasma experiments. It could be demonstrated that the prepulse energy delivered to the target is always kept at a sufficiently low level. In addition, a high beam quality is obtained without using any beam quality improving components such as spatial filters. Furthermore the pulse is found to be temporally smooth without any substructure and the pulse width can be adjusted in a wide range. Moreover it turns out that owing to the small amplification bandwidth the isolation of the laser from the target can be achieved relatively easily. And finally the maintenance effort for the Asterix III laser is low. Its operation is reliable and reproducible and its repetition rate is high.

The performance of the Asterix III system can still be further improved, and its overall efficiency, whose present value is obtained without any optimization, can therefore also be raised.

Generally speaking, the iodine laser is still not highly developed and therefore this laser affords potential for further improvements far beyond the scope of the Asterix III laser. For a system built according to our present capabilities the pumping efficiency can be improved by as much as a factor of about two using conventional means, such as more refined reflector geometries and flash lamp arrangements or flashlamps directly embedded in the laser medium. This efficiency can be further increased by a more effective pumping source. Here the prospects look promising ; however, little work has been done. The extraction efficiency of the stored optical energy can also be improved by better matching of the amplifiers and possibly by multi-line operation (both line group of the laser transition) of the system.

Regarding the scaling capability of a single beam to output energies in the several kJ range there are no restrictions /22/. Amplifiers up to an aperture of 50 cm and even more can be built. The beam loading here is only limited by the damage threshold of optical components.

Taking into consideration the economic aspects of the iodine laser, it turns out that the personnel and financial requirements for developing and constructing an iodine laser are moderate compared with the corresponding costs for other high power lasers. As also the operation costs of this laser are low and high repetition rates can be reliably achieved, the iodine laser has proved to be a highly qualified and economic tool for high power plasma experiments.

References

1 K. Hohla, K.L. Kompa, IEEE J. Quant. Electron. QE-8, (1972) 198

2 N.G. Basov, V.S. Zuev, Il Nuovo Cimento, 31 B, N. I (1976) 129

3 M.E. Riley, R.E. Palmer, Sandia Report SAND 77-0775

4 G. Brederlow, K.J. Witte, E. Fill, K. Hohla, R. Volk, IEEE J. Quant. Electron. QE-12, (1976) 152

5 E.A. Yukov, Kvantovaya Elektron., 2, (1973) 53

6 W. Thieme, E. Fill to be published in J. of Appl. Phys. D.

7 F.I. Aldridge, IEEE J. Quant. Electron. QE-11, (1975), 215

8 V.S. Zuev, V.A. Katulin, V. Yu. Nosach, and O. Yu. Nosach, Zh. Eksp. Theor. Fiz., 62, (1972) 1673

9 W. Fuß, K. Hohla, Z. Naturforsch. 31a, (1976) 569

10 T.D. Padrick and R.E. Palmer, J. Chem. Phys. 62, (1975) 3350

11 W. Fuß, K. Hohla, Opt. Comm. 18, N.4, (1976) 427

12 V.A. Gaidash, G.A. Kirillow, S.B. Kormer, S.G. Lapin, V.I. Sheminkin, V.K. Shirigin; ZhETF letters 20, (1974) 243

13 E. Fill, K. Hohla, Opt. Comm. 18, (1976) 431

14 J.N. Olsen, J. of Appl. Phys. 47 N 12, (1976) 5360

15 K.J. Witte, R. Volk, M. Nippus, PLF Report, PLF 1979 to be published

16 K.J. Witte, J. of Appl. Phys. D 12, (1979), 9

17 W.W. Simmons, D.R. Speck, and J.T. Hunt, Appl. Opt. 17, (1978) 999

18 K.J. Witte, G. Brederlow, K. Eidmann, R. Volk, E. Fill, K. Hohla, R. Brodmann, Proceedings of the "High Power Lasers and Applications Conference" June 1977, Munich; published in Series in Optical Sciences Vol. 9 (Springer).

19 K. Eidmann, G. Brederlow, R. Brodmann, R. Petsch, R. Sigel, G. Tsakiris, R. Volk, S. Witkowski, PLF Report, PLF 4/1978

20 K. Eidmann, G. Brederlow, R. Brodmann, R. Petsch, R. Sigel, G. Tsakiris, R. Volk, S. Witkowski, PLF Report, PLF 15/1979

21 L.M. Frantz, J.S. Nodvik, J. Appl. Phys. 34, (1963) 2346

22 M. Nippus, PLF Report, PLF 17/1979